ACCSCIENCE PUBLISHING

International Journal of Bioprinting

RESEARCH ARTICLE

Evaluation of a synthetic peptide-based bioink (PeptiInk Alpha 1) for *in vitro* 3D bioprinting of cartilage tissue models

Patricia Santos-Beato[1], Andrew A. Pitsillides[2], Alberto Saiani[3], Aline Miller[4], Ryo Torii[5], and Deepak M. Kalaskar[6]*

[1]Biochemical Engineering Department, University College London, London, United Kingdom

[2]Comparative Biomedical Sciences, Royal Veterinary College, London, United Kingdom

[3]Division of Pharmacy & Optometry & Manchester Institute of Biotechnology, The University of Manchester, Manchester, United Kingdom

[4]Department of Chemical Engineering & Manchester Institute of Biotechnology, The University of Manchester, Manchester, United Kingdom

[5]Department of Mechanical Engineering, University College London, London, United Kingdom

[6]Institute of Orthopaedics and Musculoskeletal Science, Division of Surgery & Interventional Science, University College London (UCL), London, United Kingdom

(This article belongs to the *Special Issue: Advances in bioprinting technology*)

Abstract

Cartilage pathology in human disease is poorly understood and requires further research. Various attempts have been made to study cartilage pathologies using *in vitro* human cartilage models as an alternative for preclinical research. Three-dimensional (3D) bioprinting is a technique that has been used to 3D-bioprint cartilage tissue models *in vitro* using animal-derived materials such as gelatine or hyaluronan, which present challenges in terms of scalability, reproducibility, and ethical concerns. We present an assessment of synthetic self-assembling peptides as bioinks for bioprinted human *in vitro* cartilage models. Primary human chondrocytes were mixed with PeptiInk Alpha 1, 3D-bioprinted and cultured for 14 days, and compared with 3D chondrocyte pellet controls. Cell viability was assessed through LIVE/DEAD assays and DNA quantification. High cell viability was observed in the PeptiInk culture, while a fast decrease in DNA levels was observed in the 3D pellet control. Histological evaluation using hematoxylin and eosin staining and immunofluorescence labeling for SOX-9, collagen type II, and aggrecan showed a homogeneous cell distribution in the 3D-bioprinted PeptiInks as well as high expression of chondrogenic markers in both control and PeptiInk cultures. mRNA expression levels assessed by - qRT-PCR (quantitative real time-polymerase chain reaction) confirmed chondrogenic cell behavior. These data showed promise in the potential use of PeptiInk Alpha 1 as a bioprintable manufacturing material for human cartilage *in vitro* models.

Keywords: 3D bioprinting; Self-assembling peptides; Bioinks; Cartilage; *In vitro*

***Corresponding author:**
Deepak M. Kalaskar
(d.kalaskar@ucl.ac.uk)

Citation: Santos-Beato P, Pitsillides AA, Saiani A, *et al*., 2023, Evaluation of a synthetic peptide-based bioink (PeptiInk Alpha 1) for in vitro 3D bioprinting of cartilage tissue models. *Int J Bioprint*, 9(6): 0899.
https://doi.org/10.36922/ijb.0899

Received: May 4, 2023
Accepted: June 27, 2023
Published Online: September 6, 2023

1. Introduction

The treatment of cartilage pathologies remains a challenge in the field of orthopedic medicine. Diseases such as osteoarthritis, rheumatoid arthritis, or post-traumatic

cartilage injuries still have no cure or 100% effective treatment. These diseases are extremely prevalent, with rheumatoid arthritis and osteoarthritis affecting 0.5%–1% of the world population[1] and 36.8% of the U.S. adult population, respectively[2]. Due to the lack of nerve signaling and vasculature in cartilage, the latter is difficult to diagnose at initial stages and has a limited endogenous repair potential. Additionally, cartilage has an extraordinarily complex structure, presenting up to four distinct articular cartilage zones[3], making it extremely difficult to replicate *in vitro*.

The superficial zone comprises collagen fibers aligned parallel to the surface and chondrocytes with an elongated shape. Beneath this is a middle zone where collagen fibers are randomized, and chondrocytes present their characteristic rounded shape. Further down, the deep zone contains collagen fibers that are perpendicular to the tide mark and rounded chondrocytes positioned in columns in the same perpendicular orientation. The deepest calcified cartilage zone contacts with bone and contains hypertrophic chondrocytes[3]. In addition to this complicated structure, the lack of vasculature forces nutrients to be distributed through diffusion[4], making tissue healing not only challenging but also a slow process. Due to these difficulties in natural regeneration, multiple studies have focused on recreating cartilage *in vitro* to use it as implants *in vivo*[5,6] or to study potential tissue regeneration methods[7,8].

Current tissue engineering techniques have been used in attempt to develop *in vitro* cartilage constructs using natural or synthetic polymer-based scaffolds that are then populated using two-dimensional (2D) cell seeding approaches. Depending on the porosity of the material, cells exhibit different colonization rates and viabilities. However, this approach has a lack of control over three-dimensional (3D) cell colonization and a lack of structural control over the scaffold itself. 3D bioprinting, a technique that enables layer-by-layer manufacture, has been used to overcome these limitations[9]. 3D bioprinting allows for multi-structural and controlled manufacturing as well as homogeneous deposition of encapsulated cells within the bioprinted structure[10]. Intricate 3D CAD (computer-aided design) designs can be made to recreate the different cartilage layers and better mimic the characteristics of this tissue. Multiple 3D printing techniques are currently used, such as extrusion-based, jetting-based, and vat photopolymerization-based. Extrusion-based technique combines a fluid-dispensing system and a robotic control system[11]. It presents advantages such as a great deposition and printing speed, affordability and a wide range of potential printing materials[11]. However, its resolution is limited, and most materials printed require to be shear-thinning[11]. Jetting-based 3D bioprinting enables contactless patterning and deposition of cell-laden biomaterials[12]. Although it is a manufacturing technique that highly facilitates cell–cell and cell–matrix interactions, it presents a limited choice of printable bioinks[12]. Vat photopolymerization-based bioprinting relies on a scanning laser that cures the photocurable bioresin in a predefined pattern[13]. This technique has a high fabrication accuracy; however, it relies on photoinitiators, which can be toxic when mixed with cells[13].

A recent systematic review[9] concluded that of the three most common cartilage 3D bioprinting techniques (extrusion-based, jetting-based, and vat photopolymerization-based), extrusion-based 3D bioprinting was the most popular[14]. According to most papers, animal-based gelatine methacrylate (GelMA)[15-23], hyaluronic acid-based[17,22,24], or chondroitin sulfate-based materials[15,24] were used. Although alginate is also one of the most commonly used materials in bioprinting, its poor cell attachment properties require that it be mixed with other GelMA, hyaluronic acid-based, and chondroitin sulfate-based materials to enhance these properties. Even though these mixed materials are widely used, they present multiple disadvantages such as low reproducibility, scalability, and low mechanical property[25,26]. Furthermore, there is a need to move toward a more sustainable and ethical approach in science, encouraged by the EU Directive 2010/63 and the Guidance Document on Good *In Vitro* Method Practices[27], hence prompting the exploration of non-animal-derived synthetic materials as a viable alternative.

Synthetic polymers can be modified to improve their mechanical and physical properties as well as to control their degradation time; these advantages also result in better reproducibility and less batch-to-batch variation. Prior studies have demonstrated the potential of synthetic self-assembling peptide hydrogels for use in cartilage studies[28-30]. Such transparent peptide materials are shear thinning and do not require crosslinking, making them perfect off-the-shelf materials for easy and accessible bioprinting. Due to their synthetic nature, there is a minimal batch-to-batch variation, which ensures reproducibility in printed structures, making them an exceptional alternative to natural materials. Preliminary studies have also shown the potential application of these self-assembling peptides in 3D bioprinting[31]. Due to the differences between hydrogel performances (synthetic or natural), it is not currently possible to define a hydrogel-based "gold standard" system for cartilage manufacturing *in vitro*. Therefore, when assessing the performance of a hydrogel for cartilage *in vitro* manufacturing, comparing it to the native tissue is preferred. Alternatively, *in vitro*

chondrocyte-based cartilage models, such as the chondrocyte 3D pellet model[32,33], can be used when native tissue explants are not available. Here, we explored peptide hydrogel bioinks, PeptiInks®, in terms of their application in 3D bioprinting using human primary chondrocytes for cartilage tissue modeling *in vitro*. We compared its performance to a control 3D chondrocyte-based pellet developed *in vitro* using previously optimized manufacturing protocol[34].

In this study, we assessed the potential of PeptiInk Alpha 1 (Manchester BIOGEL, Alderley Park, UK) as a material for 3D-bioprinting human cartilage tissue *in vitro* models. Primary human chondrocytes were encapsulated into PeptiInk Alpha 1, a neutrally charged peptide hydrogel, and 3D-bioprinted structures were manufactured. Cell viability, cell proliferation, and specific cartilage marker production were assessed and compared to the current gold standard, chondrocyte cell pellets.

2. Materials and methods

2.1. Hydrogel rheological characterization

Synthetic self-assembling peptide hydrogel Alpha 1 was obtained from Manchester BIOGEL (Alderley Park, UK). Alpha 1 was chosen due to its neutral charge, which has previously been shown to promote the chondrogenic behavior of bovine chondrocytes in 3D *in vitro* cultures[28-30] and has a compressive modulus (E = 31 kPa[29]) in line with previously used hydrogels for cartilage tissue engineering[16,24] .

Oscillatory shear rheometry was performed using a Kinexus pro+ rheometer (Netzsh, Germany) with parallel sandblast plate geometry (40 mm, 0.5 mm gap size), equilibrated to room temperature (25°C), and a solvent trap to prevent the hydrogel from drying. Alpha 1 alone and Alpha 1 mixed with cell culture media in a 1:10 ratio were tested in triplicate to ensure reproducibility. For all mixtures, rotational shear-viscosity measurements were performed. Flow sweeps at 1% strain with a shear rate ranging from 150 to 1 Hz were performed to assess the viscosity behavior under shear stress.

2.2. Printability tests

Alpha 1 was loaded into a printer cartridge and printed, using the BIOX6 bioprinter (CELLINK, Sweden), with multiple gauge (G) conical nozzles: 22G (400 μm—extrusion diameter), 25G (250 μm—extrusion diameter), and 27G (200 μm—extrusion diameter). 25G conical nozzle was chosen as it gave a compromise between structural accuracy and shear stress production. Different pressures and printing speeds were combined to assess the filament continuity and width of Alpha 1 printed with a 25G conical nozzle. Images of the printed structures were taken with an EVOS microscope to quantify the filament width using Fiji ImageJ software (1.53t version). Six images were taken at different locations within the printed structure. In each image, the filament width was quantified three times using ImageJ and compared to the theoretical filament resolution.

2.3. Cell culture

Human primary chondrocytes (HCHs; CellApplications, San Diego, CA) were used in this study. HCHs between passages 5 and 7 were consistently used. HCHs were cultured in chondrogenic growth media (Cell Applications, San Diego, CA), and they were incubated at 37°C in a humidified atmosphere with 5% pCO_2. The media was changed every 2 to 3 days.

2.4. Hydrogel cell encapsulation

HCHs were manually mixed into Alpha 1 at a concentration of 1×10^6 cells/mL using a ratio of 1 mL of PeptiInk to 100 μL of cell culture media (1:10). Cell-laden PeptiInks were loaded into 3-mL printing cartridges (Nordson, USA) using a positive displacement pipette (Gilson Scientific, Dunstable, UK). Loaded cartridges were centrifuged to remove air microbubbles for 2 min at 3500 rpm and immediately printed into 12-well culture plates.

2.5. 3D bioprinting of HCH cell-laden Alpha 1

The 3D-bioprinting process was performed using the commercial printer BIOX6 (CELLINK, Sweden). Cylindrical structures with an outer diameter of 5 mm and a thickness of 1 mm with 60% infill density were bioprinted using a 25G conical nozzle, an extrusion pressure between 8 and 10 kPa, and a printing speed of 5 mm/s. The printed structures were submerged in chondrogenic medium, which was changed three times during the first hour to ensure pH equilibrium and twice each week over the culture period. Cell constructs were cultured for up to 14 days at 37°C in a humidified atmosphere with 5% pCO_2.

2.6. Cell pellet formation and culture

3D control cell pellet cultures were formed using the methods of Yeung *et al.*[34] Briefly, 4×10^5 cells were centrifuged in 500 μL of culture media at 1750 rpm for 5 min in 15 mL tubes. After 72 h, the pellets were gently aspirated into ultra-low adhesion 24-well plates (ScienceCell, 0383), with one pellet per well cultured in 1 mL of chondrogenic medium. Culture media were changed every 2 to 3 days. The cell pellets were cultured for up to 14 days at 37°C in a humidified atmosphere with 5% pCO_2.

2.7. Cell viability

Cell viability was assessed using a LIVE/DEAD assay. Bioprinted constructs were assessed 2 h post-printing (day 0), on day 7 and day 14. Samples were cut in half to enable the

visualization of cell viability in the center of the constructs. Samples were washed twice with phosphate-buffered saline (PBS; Gibco, 20012-019) and then incubated at 37°C for 30 min in LIVE/DEAD cytotoxicity assay (Invitrogen, L3224) using a concentration of 5 µL of calcein-AM and 20 µL of ethidium homodimer per 10 mL of PBS (Gibco, 20012-019). After incubation, constructs were rinsed twice using PBS (Gibco, 20012-019) and imaged using an Olympus DP80 microscope. Multiple z-stacks were taken at magnifications of 10× and 20× using FITC (488 nm) and TRITC (532 nm) filters. Semi-quantitative evaluation of cell viability was performed using Fiji Image-J software (1.53t version). In summary, red and green image channels were separated, and three random regions of interest were selected to perform manual cell counting. Average cell survival percentages for each time point were calculated and compared to 3D controls; dead and live cells were counted at each specific time point and not used for comparison between time points due to the cell viability not being cumulative.

2.8. DNA quantification

DNA quantification was assessed using a Quant-iT PicoGreen dsDNA Assay Kit (Thermo Fisher, P7589). Bioprinted constructs and 3D cell pellets were mixed with pre-warmed (37°C) protease solution (10 mg/mL) (Sigma Aldrich, P5147-1G) and pipetted up and down until the PeptiInk or cell matrix was dissolved. This mixture was then incubated at 37°C for 5 min. Sequentially, these samples were mixed with 500 µL of 2× TE Buffer from the Quant-iT PicoGreen dsDNA Assay Kit (Thermo Fisher, P7589), and 1% Triton X in UltraPure™ DNase/RNase-Free Distilled Water (Thermo Fisher, 10977-035). Mixtures were incubated at 37°C for 30 min and then placed at -20°C. Samples were subjected to three freeze-thaw cycles before the assay was performed. PicoGreen dye was diluted (1:200) in 2× TE buffer. A total of 100 µL from each sample was pipetted in a black/opaque 96-well plate. An additional 100 µL of the PicoGreen dye solution was then added and left for 5 min under constant mixing at room temperature. Fluorescence was immediately measured using a plate reader at excitation and emission wavelengths of 480 nm and 520 nm, respectively, for DNA concentration calculation. Change in DNA concentration was calculated against concentration at day 0 (100%).

2.9. Histological processing and cryosectioning

3D cell pellets and bioprinted constructs were washed with PBS (Gibco, 20012-019) for 5 min at different time points (days 0, 7, and 14) and then fixed overnight at 4°C in a 10% neutral buffered formalin solution (Sigma Aldrich, HT501128). After fixation, samples were washed for 5 min in PBS and then left for 3 h in 30% sucrose (Sigma Life Sciences, S9378) solution in PBS (Gibco, 20012-019) to dehydrate. They were then submerged in a 50:50 ratio mixture of 30% sucrose solution and OCT mounting media (VWR chemicals, 361603E) overnight at 4°C. Samples were then placed in cryomolds filled with OCT (VWR chemicals, 361603E), snap-frozen in liquid nitrogen, and cryosectioned at 8 µm using a ThermoScientific cryotome FSE for further immunohistochemistry processing.

2.10. Hematoxylin and eosin staining

Routine hematoxylin and eosin (H&E) staining of bioprinted constructs and 3D cell pellets sections were conducted at time points: days 0, 7, and 14 on the cryosections. Excess OCT was removed by submerging the slides in 70% ethanol. Hematoxylin staining was performed for 10 min, and subsequently, Scott's water was used to ensure nuclei bluing. Eosin staining was done for 15 s, followed by washing in 70% ethanol.

2.11. Immunofluorescence labeling

Cryopreserved sample sections were rehydrated for 10 min with PBTD (PBS + 1.1% DMSO + 0.1% Tween 20) and subsequently fixed for 10 min using 10% neutral-buffered formalin (Sigma Aldrich, HT501128). Sections were then blocked for 1 h at room temperature using PBTD and 5% bovine serum albumin (BSA; Sigma Aldrich, A2153).

Primary antibody incubation was performed overnight at 4°C, and the slides were kept in a humidity chamber. Collagen type II primary antibody (Invitrogen, PA1-36059) was diluted at a ratio of 1:50; aggrecan primary antibody (Abcam, ab3778) was diluted at a ratio of 1:100; SOX-9 primary antibody (Abcam, ab185966) was diluted at a ratio of 1:100 in PBTD and 5% BSA solution. All sections were washed in PBS for 5 min after primary antibody labeling was performed.

Secondary antibody incubation was performed at room temperature. For collagen type II labeling, secondary antibody AlexaFluor-488 goat anti-rabbit (Invitrogen, A11008) was incubated for 1 h at a ratio of 1:200 combined with phalloidin (Invitrogen, A12381) at a ratio of 1:200 in PBS. Aggrecan labeling was performed with the AlexaFluor 594 goat anti-mouse secondary antibody (Abcam, ab150116) diluted at a ratio of 1:200 for 3 h in PBS. SOX-9 labeling was performed with AlexaFluor 555 goat anti-rabbit (Invitrogen, A21428) incubated for 1 h at a ratio of 1:200 in PBS. All sections were then washed for 5 min in PBS, and nuclei staining was performed by incubating the sections for 3 min at room temperature with DAPI (Thermo Fisher, 62248) diluted at a ratio of 1:200 in PBS. Further section rinsing was done for 5 min in PBS, before section mounting with fluoroshield (Sigma Aldrich, F6182).

Table 1. Primer sequences used in the comparative PCR

Gene	Forward sequence 5'-3'	Reverse sequence 5'-3'
GADPH	GGAGCGAGATCCCTCCAAAAT	GGCTGTTGTCATACTTCTCATGG
COL2	GGATGGCTGCACGAAACATACCGG	CAAGAAGCAGACCGGCCCTATG
AGC	AACCACCTCTGCATTCCACG	CCTCTGTCTCCTTGCAGGTC
SOX9	GGCGGAGGAAGTCGGTGAAGAA	GCTCATGCCGGAGGAGGAGTGT

2.12. RNA extraction and polymerase chain reaction

RNA extraction of the hydrogel cultures was performed by washing the hydrogels three times with PBS and digesting the hydrogel for 5 min at 37°C using a protease solution (10 mg/mL in distilled DNAse-free, RNAse-free water). To initiate RNA extraction, the digested mixture was mixed with the RNeasy lysis buffer from the QIAGEN RNeasy Mini kit (74104, QIAGEN) by centrifugation at 10,000 rpm for 3 min. The following steps were performed as specified by the RNA extraction kit's manufacturer. RNA extraction of the 3D cell pellets was performed as specified by the RNA extraction kit's manufacturer (QIAGEN). mRNA levels were quantified using a Nanodrop spectrophotometer. cDNA was obtained using the High-Capacity RNA-to-cDNA Kit (ThermoFisher, 4387406) according to instructions specified by the manufacturer.

Gene expression levels of collagen type II (*COL2*), aggrecan (*AGC*), and SOX-9 (*SOX9*) were analyzed by comparative polymerase chain reaction (PCR) using *GADPH* as a housekeeping gene. Primer sequences are reported in Table 1. The comparative cycle threshold (CT) method, using the expression levels at day 7 and day 14 of the 3D cell pellet as the reference respectively for the $2^{-\Delta\Delta Ct}$ calculation, was used to calculate the gene expression fold of change.

2.13. Statistical analysis

GraphPad Prism 9 was used for the graphical representation of data and statistical analysis. All graphs show error bars, which represent standard deviation. For DNA quantification and percentage DNA change, two-way analysis of variance (ANOVA) was performed. For PCR analysis, multiple unpaired *t* tests with Mann–Whitney test were performed. Statistical significance was calculated with a confidence interval of $p < 0.05$.

3. Results

3.1. Characterization of the inks and bioprinting optimization

The PeptiInk Alpha 1 bioink was characterized rheologically by measuring changes in viscosity as a function of shear stress. As this bioink requires to be mixed with cell culture media for 3D-bioprinting cell-laden structures, both pure Alpha 1 and Alpha 1 mixed with culture medium (1:10 medium-to-gel ratio) were characterized. Viscosity for both decreased with increases in shear stress (Figure 1A), confirming the expected shear thinning behavior. Comparison revealed that when mixed with cell culture medium, the viscosity is lower than the Alpha 1 alone at low shear stress and higher at frequencies above 10 Hz. This was expected as previous work[35] has demonstrated the increase in compressive modulus when self-assembling peptides were mixed with culture media.

Further visual characterization was performed by assessing changes in the deposited filament with respect to the conical nozzle size used. 22G, 25G, and 27G nozzles were used to 3D-print a 30 × 30 mm grid (Figure 1B). Continuous filament deposition was observed when using all conical nozzle sizes. Filament width was quantified, and the expected decrease in filament width with respect to decreasing nozzle size was observed (Figure 1C). The 25G conical nozzle was chosen and used in an attempt to find a compromise between the filament deposition resolution and the shear stress generated. Smaller nozzle sizes have been proven to result in higher levels of cell death due to shear stress[36]. The filament width with respect to extrusion pressure and printing speed was further investigated in 25G nozzles. As seen in Figure 1D, a range of pressures from 6 to 12 kPa were selected to print a simple shape at a constant printing speed of 10 mm/s using a 25G conical nozzle. At low 6 kPa pressures, the ink presented a discontinuous filament deposition behavior, whereas at higher 12 kPa pressures, an excess of bioink deposition was observed, engendering adjacent filament fusion. An intermediate range of pressures (8–10 kPa) was chosen as the working extrusion pressure range as the deposited filaments were continuous and there was no filament fusion observed.

Additional characterization involved quantification of filament width of the structures printed at different printing speeds. The printing was performed with a 25G conical nozzle and the pressure range previously selected. Using Fiji ImageJ software (1.53t version), the filament width was quantified and plotted. The images obtained of the filaments can be found in **Figure S1** (Supplementary File). As seen in Figure 1E, the expected decrease in filament width with increasing printing speed was observed at the

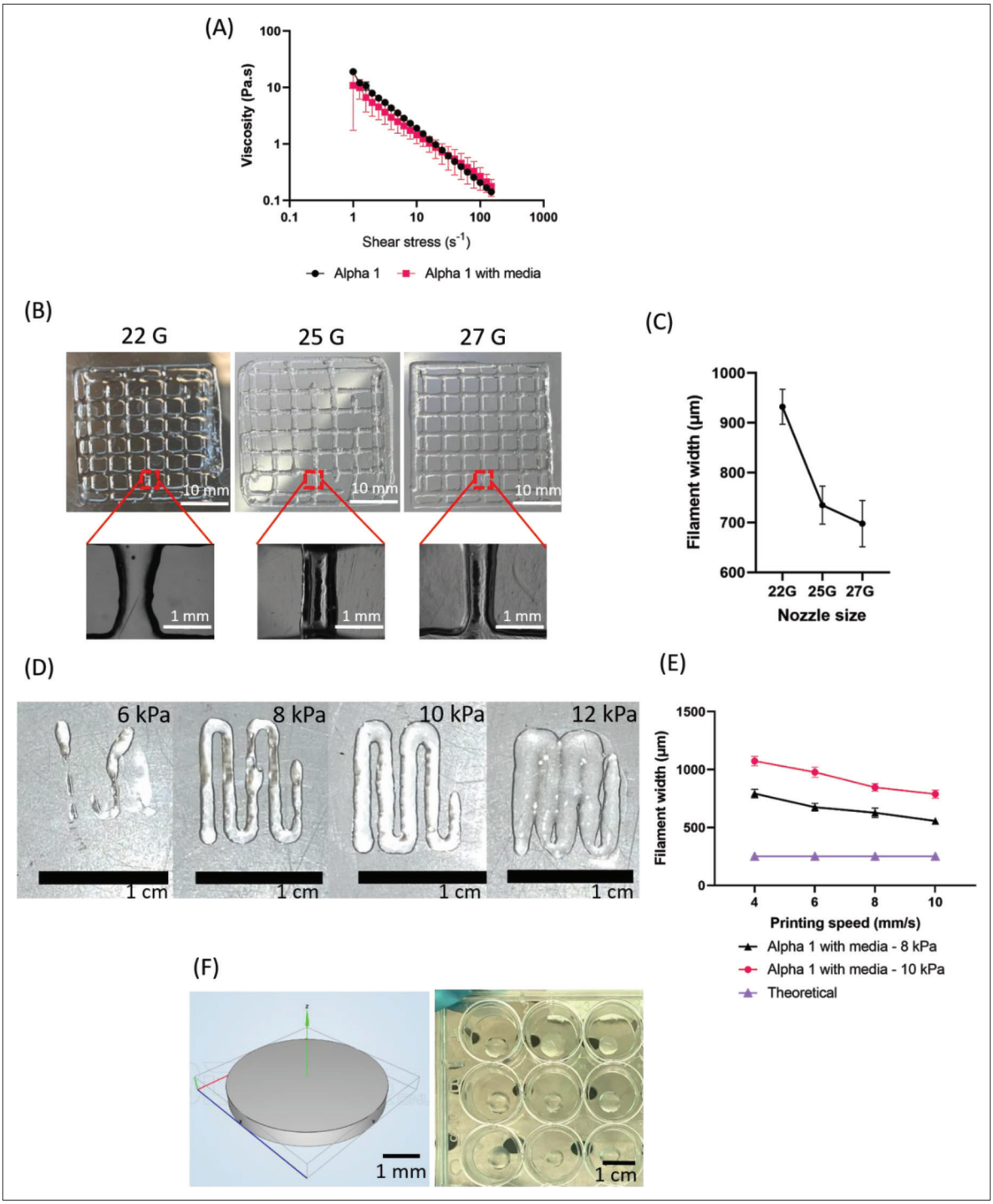

Figure 1. Optimization of 3D printing process for Alpha 1. (A) Dynamic viscosity vs. shear stress for Alpha 1, with and without medium (1:10). $N = 3$; error bars show standard deviation. (B) Initial typical images of 3D-printed grid structure (30 × 30 mm) produced by different conical nozzle sizes (400 µm—22G, 250 µm—25G, and 200 µm—27G). (C) Quantification of the printed filament width of Alpha 1 using different nozzle sizes. $N = 3$; error bars show standard deviation. (D) Typical images of printed Alpha 1 filaments at different extrusion pressures at constant printing speed of 10 mm/s using a 25G conical nozzle. (E) Correlation of printing speed with filament width at extrusion pressures of 8 and 10 kPa. (F) CAD design of printed cylindrical structures (5 mm diameter, 1 mm thickness with 60% infill density) and images of printed structures in a 12-well plate.

two selected pressures. Comparison to theoretical filament width, which corresponds to an internal nozzle diameter (250 μm, 25G), was also performed. This showed a high shape fidelity and printing consistency, with a low standard deviation and high reproducibility (Figure 1E). Although higher printing speeds approached the theoretical filament width when printed at 8 kPa, a more conservative printing speed was chosen to develop the targeted structures to avoid printing inconsistencies. A pressure range of 8–10 kPa and a printing speed of 5 mm/s were selected when printing with the 25G conical nozzle. A compact cylindrical shape structure was chosen to 3D-bioprint the *in vitro* cartilage tissue models (Figure 1F). These models had a 5 mm diameter, 1 mm thickness, and 60% infill density.

3.2. Establishing cellular viability post-printing in short- and long-term culture

Viability of cells in constructs was assessed post-printing with calcein-AM (alive) and ethidium homodimer (dead). Post-printing cell viability and material cytocompatibility were studied to evaluate the effect of the extrusion process on cell viability. For this, human primary chondrocytes were encapsulated in the PeptiInk and bioprinted. Cell viability was assessed 2 h after extrusion and on days 7 and 14 of culture, using cell pellet cultures as the control. Pellet cultures showed 100% viability at day 0, 2 h after centrifugation, which was significantly decreased ($p < 0.0001$) to 46% at day 7 (Figure 2A) with a high number of dead cells in the pellet core, and similar viability (54%) was found at day 14. The cell death observed in the 3D pellet culture was expected as it has been previously reported that hypoxic conditions lead to a necrotic core[37]. In contrast, cells in Alpha 1 PeptiInk showed a 30% viability post-printing, with significant increases to 59% by day 7 and remaining stable (59%) thereafter until day 14. Cell number changes assessed by DNA quantification showed that the 3D pellet control exhibited a high starting DNA quantity (58.5 ng/mL), which significantly decreased over the 14 days (by 75%, Figure 2B). Behavior of cells in Alpha 1 differed, with significant decreases in DNA content (40%) over the first 7 days but only a further 10%, non-significant decrease by day 14, confirming that DNA levels were maintained during the second week of culture in Alpha 1, which corresponds to the cell viability previously reported[29,31,35].

3.3. Extracellular matrix formation, cell morphology, and cell distribution analysis

H&E staining used to assess extracellular matrix (ECM) production, cell morphology, and distribution shows homogeneous cell distribution and circular cell shape across the bioprinted Alpha 1 hydrogel constructs on day 0. Cell distribution homogeneity demonstrated efficiency in the bioprinting process. We observed that the cells adopted a typical chondrogenic rounded morphology. Migration of the cells toward the surface of the Alpha 1 hydrogel was observed over the culture time, with cells forming clusters, which became even more prominent by day 14 (Figure 3). In these cell clusters, a change in the cell morphology from rounded to more spread out can be seen. A higher eosin staining intensity was observed within these clusters, showing a higher level of ECM secretion. Single cells that are distributed across the gel and not in the cell pellets retained their rounded morphology and had low levels of ECM around them. The 3D pellet showed a circular cell morphology and had high levels of eosin staining in the inter-cellular spaces as seen in Figure 3, indicating the presence of ECM. Across the two time points observed, there was a decrease in number of nuclei observed at the center of the pellet, suggesting some level of cell death at the core of the cell cluster, and further confirming the previously reported behavior in 3D pellets[37].

3.4. Cartilage-specific protein marker analysis

Chondrocyte differentiation was assessed by immunofluorescence for specific markers. Labeling for the early chondrogenic marker, SOX-9, was performed to investigate whether primary cells adopted a chondrogenic phenotype. It revealed positive labeling in cell nuclei in both the 3D pellet and the Alpha 1 systems on days 7 and 14. The intensity of the SOX-9 labeling was increased on day 14 in Alpha 1 in comparison to day 7. In contrast, the intensity decreased in the cell pellet culture (Figure 4). An increase of SOX-9 over 14 days of culture was expected, and it has been previously reported that the SOX-9 expression increased in chondrocytes in the first 7 days of 3D culture post 2D expansion[38]. Here, we assessed the expression beyond the 7 days to explore if the increase of expression was maintained at later time points; this increase in SOX-9 expression and maintenance in the PeptiInk culture is important to discriminate between dedifferentiation of embedded chondrocytes and potential osteoblast redifferentiation processes[39]. Decreases in SOX-9 expression in the 3D pellet culture show that chondrogenic behavior observed *in vivo*[39] is not evident. Negative controls can be found in **Figure S2** (Supplementary File).

Later chondrogenic markers, collagen type II and aggrecan, were also assessed by immunochemistry. The 3D pellet control showed an increase in collagen type II expression from day 7 to day 14, appearing firstly at the surface of the pellet and then expanding all around the

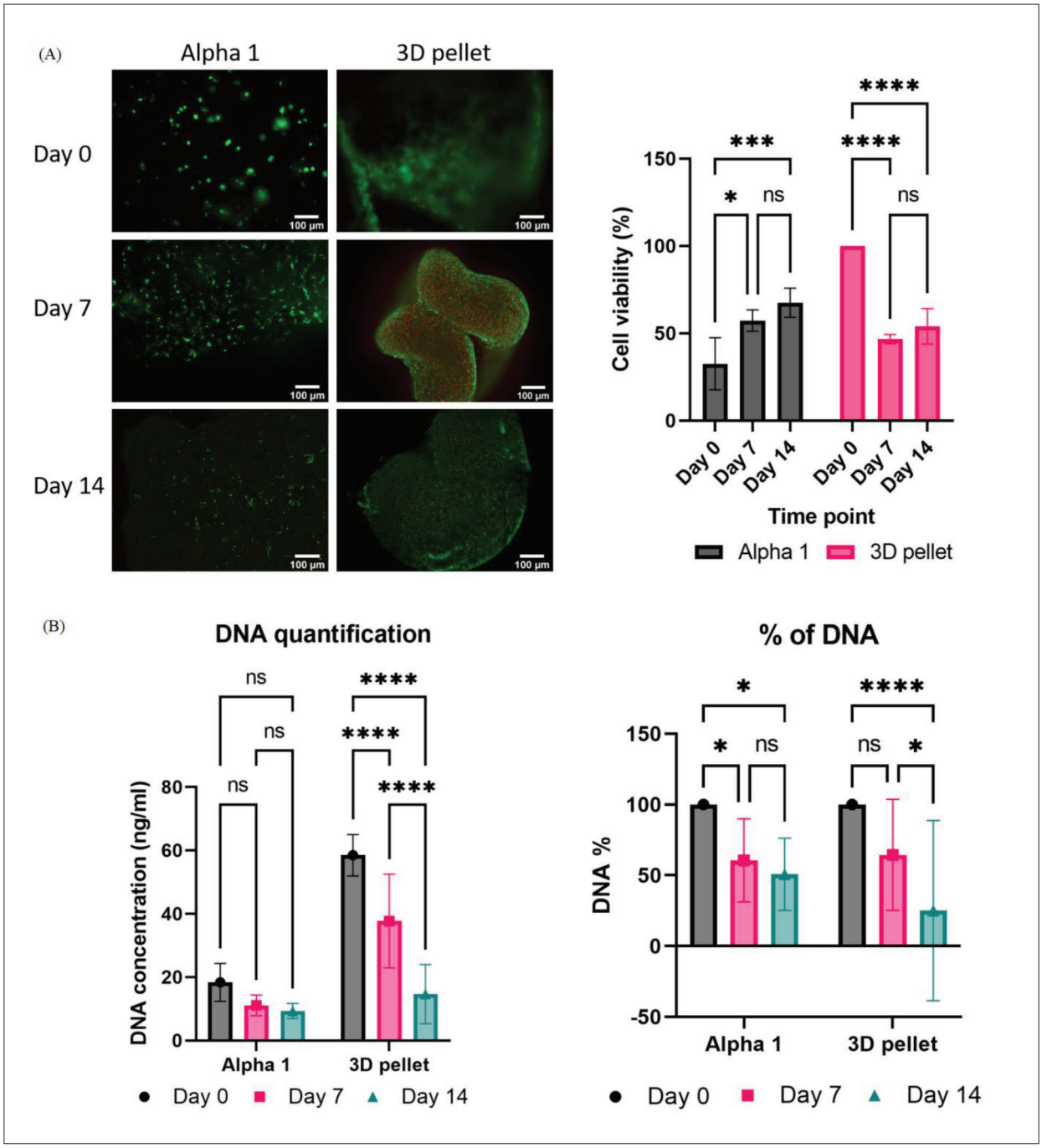

Figure 2. (A) Left: Representative LIVE/DEAD staining images obtained for 3D pellet and the PeptiInk Alpha 1 culture system at days 0 (post-printing), 7, and 14. Right: Semi-quantification of cellular viability based on cell counting of LIVE/DEAD images. (B). Left: Extracted DNA quantification obtained for 3D pellet and the PeptiInk Alpha 1 culture systems over 14 days. Right: Percentage change of DNA with respect to day 0. $N = 9$; error bars show standard deviation. Notes: ns, not significant; *$p < 0.05$; ***$p < 0.001$; **** $p < 0.0001$.

pellet matrix (Figure 5), which differed from previously reported investigations where collagen type II appeared in the center and spread out on day 7[40]. However, day 14 observations appeared to have a similar level of collagen type II expression reported in previous literature[40]. Alpha 1 showed intracellular expression of collagen type II, which increased and appeared more prominently in the surface cell clusters (Figure 5). Aggrecan expression in the 3D pellets seemed to be constant over time, showing high levels of expression both at the surface and the matrix of the pellet.

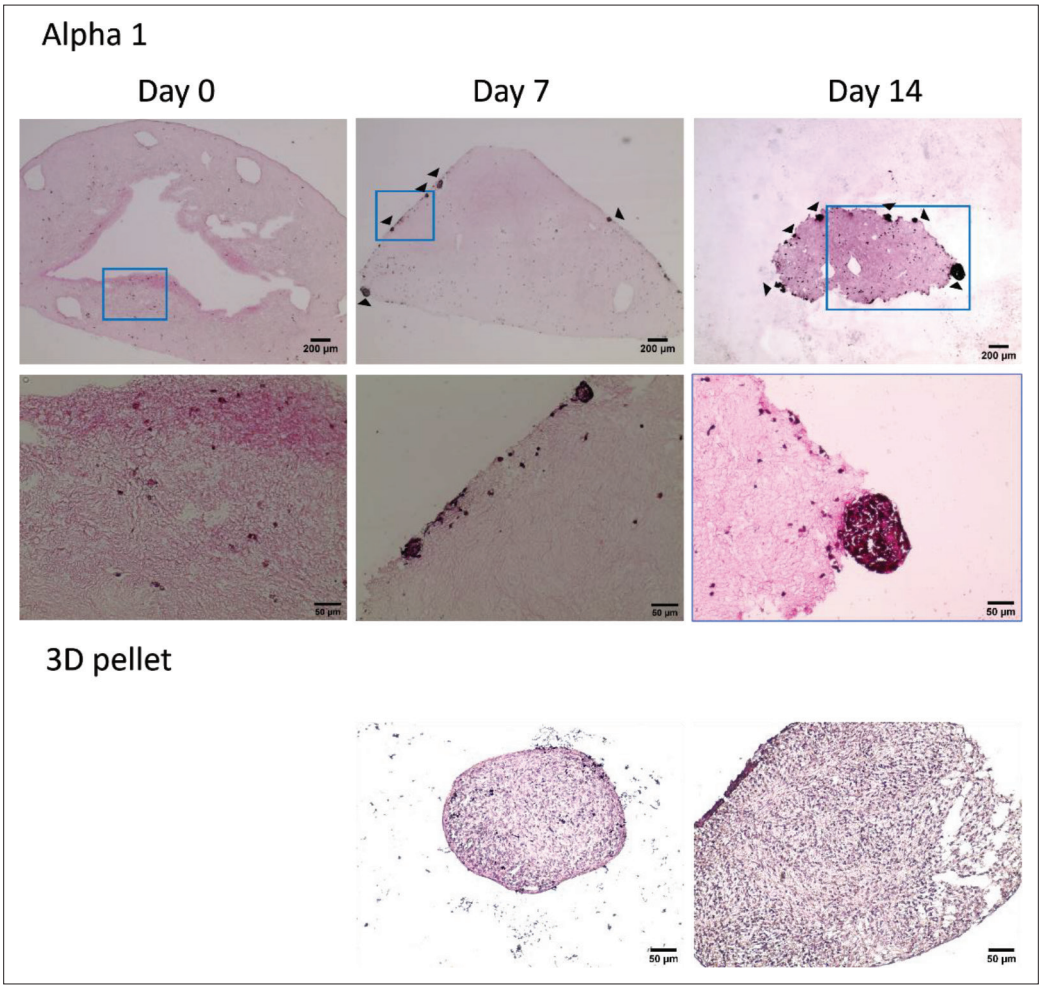

Figure 3. Top: PeptiInk Alpha 1 H&E staining. The top row shows lower-magnification images of cell-embedded hydrogels (scale bar: 200 µm); the arrows on the lower-magnification images show cell cluster formations on the PeptiInk surface. The bottom row shows the magnified sections indicated by blue boxes in the top row images (scale bar: 50 µm). Bottom: H&E staining of the 3D chondrocyte pellet over days 7 and 14 (scale bar: 50 µm).

The PeptiInk system showed low levels of intracellular aggrecan on day 7, which then increased, especially at the surface cell cluster formations (Figure 5). Negative controls can be found in **Figure S3** (Supplementary File).

3.5. PCR analysis of chondrogenic markers

In qRT-PCR, *GADPH* was used as housekeeping gene, and 3D pellet cultures were used as controls. Expression of specific cartilage markers, such as *SOX9*, *COL2,* and *AGC*, was assessed. Cells in control pellet cultures showed no significant changes in COL2, *AGC,* or *SOX9* mRNA expression from day 7 to day 14 (Figure 6A). In contrast, cells in Alpha 1 cultures showed an upregulation of all three mRNAs when compared to their corresponding control each time point (Figure 6B and C). Cells maintained in the Alpha 1 culture system exhibited a significant upregulation of *COL2*, *AGC,* and *SOX9* mRNA expression on day 7 (Figure 6B). On day 14, all mRNAs assessed were somewhat upregulated but not statistically significantly (Figure 6C).

4. Discussion

The development of human *in vitro* models is crucial to the further understanding of cartilage and diseases that affect it. Additionally, there is a need to move away from animal models, which are not necessarily always representative of human pathophysiology. Current 3D-bioprinted models rely on the use of animal-derived materials such as gelatine or hyaluronan. These are natural bioinks that present multiple advantages such as enabling cell attachment and functionalization. However, they are animal-derived bioinks, which not only give rise ethical and sustainability issues in their production but also can interfere uncontrollably within the system. The use of synthetic materials enables the possibility of creating a

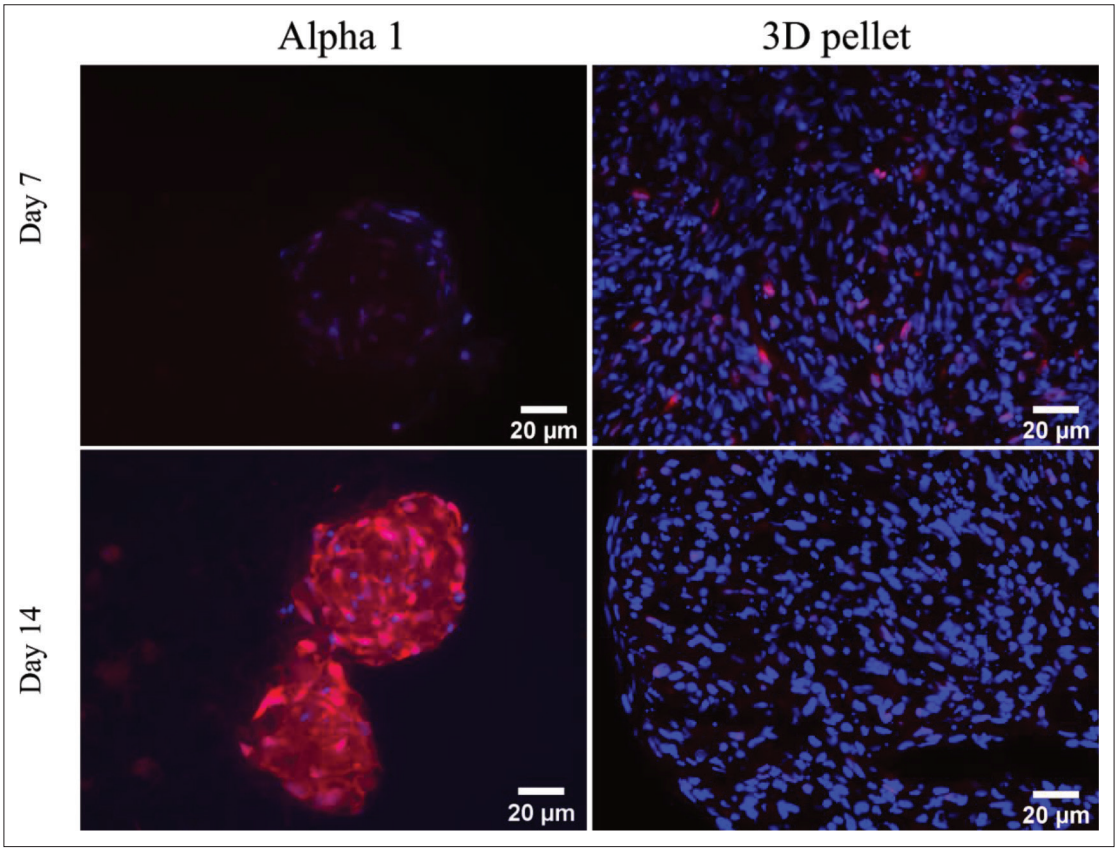

Figure 4. SOX9 (red) and cell nuclei stained with DAPI (blue) over days 7 and day 14 of culture in Alpha 1 and 3D pellet control cultures.

fully controllable and tunable environment with which we can develop cartilage human tissue models. Synthetic self-assembling peptide hydrogels have previously been used to culture animal chondrocyte-based tissue models[35]. Their potential for use as a bioink and also their application in 3D bioprinting remains unexplored. Existing models rely on tissue engineering techniques such as 2D cell seeding, which can lead to heterogeneous and uncontrolled cell deposition. Here, we embrace the advantages of 3D bioprinting, and we assess the material use in both 3D bioprinting and production of human cartilage *in vitro* tissue models.

Firstly, the rheology of the PeptiInk *Alpha 1* was assessed with and without the addition of media. As expected, the addition of medium made the hydrogel less viscous under low shear stress, enabling a better shear thinning behavior for 3D printing. However, surprisingly, at higher shear stresses, the viscosity appeared to increase. Previous work had reported the slight increase in compressive modulus of this self-assembling peptide when mixed with culture medium[35]. The addition of cell culture medium is expected to change the pH of Alpha 1 and introduce higher amounts of ions in the Alpha 1 (PeptiInk), promoting higher levels of crosslinking and an increase in compressive modulus[35]. The changes in viscosity observed when applying higher stresses could be due to the increase in crosslinking degree as time progresses when the rheological measurement is performed. In the rheological assessments, since low shear stresses have been applied before, the PeptiInk has had lesser time to crosslink. Further to characterizing its rheology, an initial bioprinting assessment was performed to visually assess any differences in filament deposition when using different nozzle sizes (22G, 25G, and 27G). No differences in terms of filament continuity were observed; therefore, the mid-size nozzle, 25G, was chosen. This choice allowed for a higher filament resolution than the 22G nozzle, but a lower shear stress was expected to be generated in smaller sizes[36], such as the 27G nozzle. Visual assessment of 25G-printed structures was performed to narrow down the extrusion pressure window using a constant printing speed of 10 mm/s. This initial screening pinpointed a pressure range of 8–10 kPa, which demonstrated the continuous deposition of the printing filament avoiding the fusion of adjacent filaments. Further optimization was required to understand the resolution of the bioink. The effect on filament width of multiple printing speeds was assessed at a constant pressure within this range, and compared to

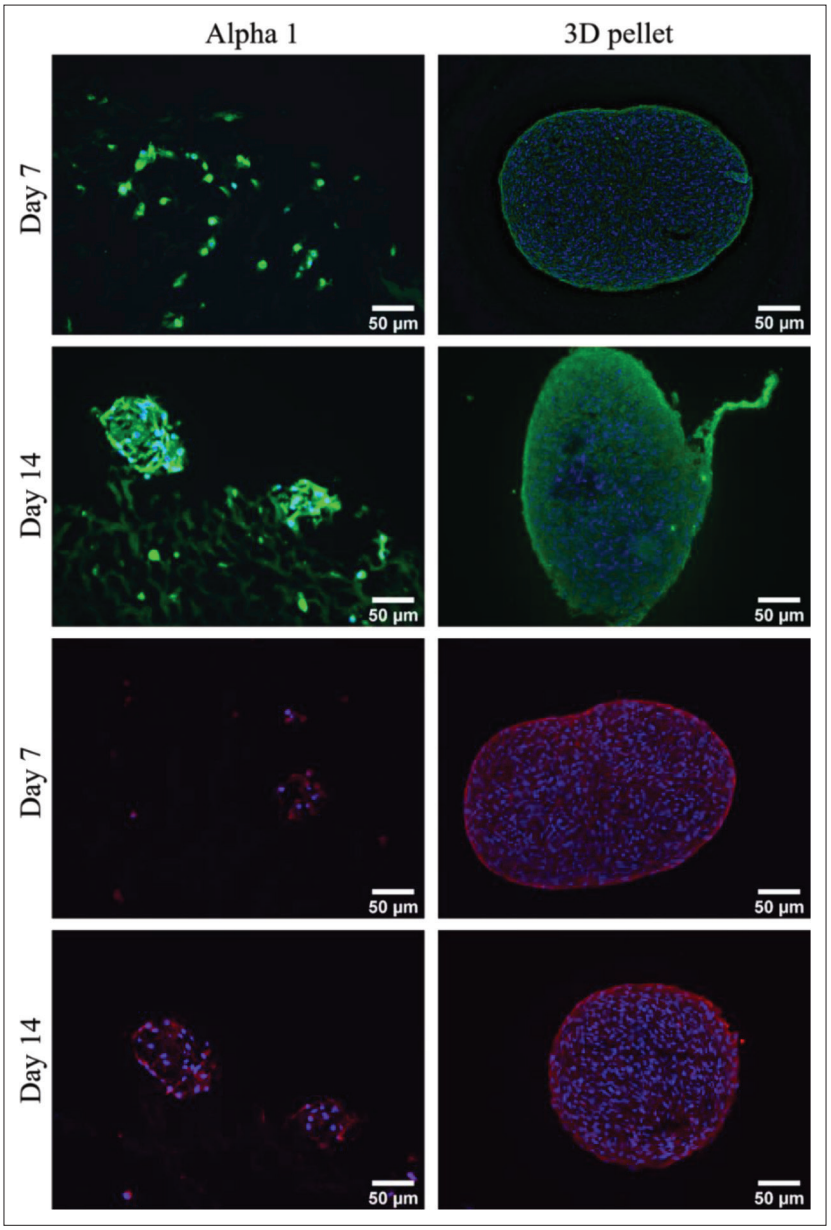

Figure 5. Top: Collagen type II staining (green) and cell nuclei staining with DAPI (blue) in 3D chondrocyte pellet and PeptiInk Alpha 1 at days 7 and 14. Bottom: Aggrecan staining (red) and cell nuclei staining with DAPI (blue) of 3D chondrocyte pellet and PeptiInk Alpha 1 at days 7 and 14.

the theoretical filament width, which corresponds to the printing nozzle diameter. As expected, the higher was the printing speed, the thinner was the deposited filament, and the closer was the resolution to the theoretical optimal value. Although the printing speed of 10 mm/s at 8 kPa of pressure showed the best printing resolution, a lower printing speed was chosen for the final manufacturing of the constructs to avoid potential printing issues. Due to the constant pressure changes that the printer experienced when moving from one well to another within the well plate, a slower printing speed enabled the printer user to manually change the printing pressure, within this window, to avoid loss of structural consistency. Higher printing speeds did not allow for consistent and fast-enough pressure changes that would ensure the required structural integrity. 3D bioprinting as the preferred choice of manufacturing technique overall demonstrated ease of use, consistency when manufacturing these constructs, and the possibility of scaling up this manufacturing process to produce more 3D-bioprinted constructs for future cartilage modeling *in vitro*.

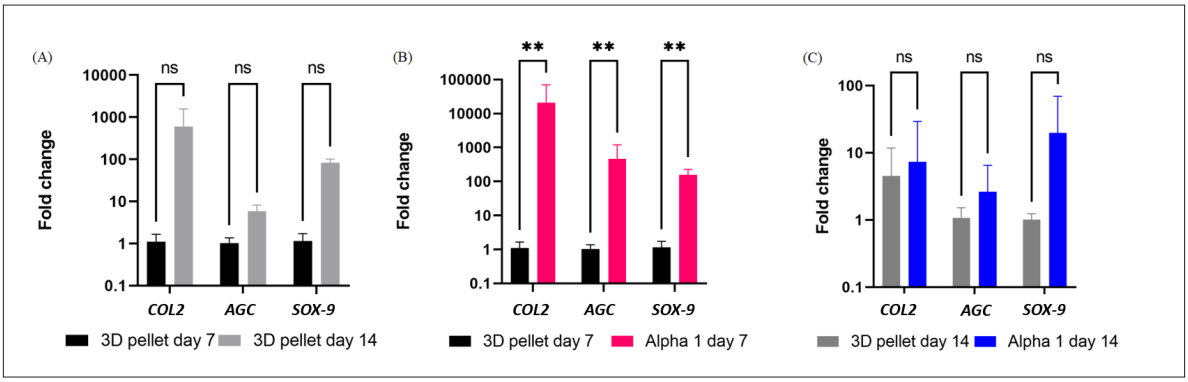

Figure 6. Fold change relative expression of cartilage markers collagen type II (*COL2*), aggrecan (*AGC*), and SOX-9 (*SOX9*) with respect to expression of housekeeping gene *GADPH*. (A) Fold change of these genes for the 3D pellet control with respect to the control on day 7. (B) Fold change of these genes for Alpha 1 on day 7 with respect to the 3D control pellet on day 7. (C) Fold change of these genes for Alpha 1 on day 14 with respect to the 3D control pellet on day 14. $N = 3$ for the 3D pellet controls; $N = 9$ for the Alpha 1 cultures. The error bars show the standard deviation of the fold change. Notes: ns, not significant; $^{**}p < 0.01$.

Secondly, once the printing optimization was achieved, multiple assessments of the capability of this material to be used as a bioink for cartilage *in vitro* tissue modeling were performed. All results were compared to a 3D chondrocyte pellet culture system, which has been widely used previously as a cartilage *in vitro* tissue system[33,40-43]. Initially, a cytocompatibility assessment of PeptiInk *Alpha 1* and viability of the 3D pellet culture was performed semi-quantitatively through live/dead staining and quantitatively through DNA quantification. The initial live/dead staining showed that cells that were in the 3D pellet configuration were almost 100% viable, confirming that the cells that were expanded in 2D pellet configuration had high viability. Across the 14 days of culture, the 3D pellet showed a 46%–54% decrease in cell viability as expected. Previous literature shows that when using this "gold standard" in *in vitro* cartilage tissue modeling, a necrotic core is formed at the center of the pellet, most likely due to hypoxia[37]. The cell viability of *Alpha 1* was assessed 2 h post-printing which showed a 30% cell viability. This low viability increased to 59% from day 7 onward (see Figure 2A), and although the printing process compromised the cell viability in the first 24 h, cells quickly recovered in the first 7 days and maintained their viability thereafter. The cell death observed in the control pellet in the first 7 days was avoided in the hydrogel culture, where the diffusion of oxygen and nutrients appeared to be more efficient as fewer dead cells were observed at the center of the hydrogel.

This cell viability was further corroborated through DNA quantification. As expected, both 3D systems showed high levels of DNA on day 0, but these significantly decreased on day 7 and further on day 14. The decrease of this DNA content in the 3D pellet coincides with the observed necrotic core, and it corresponds with observations reported in previous research[40]. *Alpha* 1 showed a non-significant decrease in DNA content over the 14 days of culture. The DNA percentage change shows a significant decrease from day 0 to 7 and from day 0 to 14. However, changes in DNA percentage between days 7 and 14 were not significant, showing the maintenance of cell numbers. It is worth noting that this could be due to the instability of the hydrogel. Over the 14 days, the volume of the hydrogel decreased, making it impossible to extend the cell culture for longer than 14 days. This degradation led to multiple cells migrating and expanding at the bottom of the well plate. However, a large number of cells remained in the hydrogel. Due to this hydrogel instability, it is not possible to state that cell number and DNA content were decreasing in the hydrogel culture, because of the lack of constant PeptiInk volume.

This degradation was not only observed visually during the culture period but also captured by histology and H&E staining, which enabled the visualization of changes in cell morphology, distribution, matrix deposition, and hydrogel dimension. The H&E staining in the 3D pellet control system illustrated the expected spherical cell morphology and high ECM deposition shown by high levels of eosin staining. Additionally, the reported cell death at the pellet core was also observed as a lower number of stained nuclei. Culture in *Alpha 1* discloses different cell and material behaviors. First, it depicts degradation of the hydrogel that occurs from day 0 up to day 14 in culture. As shown in Figure 3, the hydrogels showed a smaller cross-section which translated into a smaller overall hydrogel volume. Additionally, this showed the homogeneous distribution of cells within the gel at day 0, confirming the controlled cell deposition that was expected from using 3D bioprinting as a manufacturing technique. Secondly, a change in cell morphology and distribution was observed over the

14 days of culture with cells, which initially adopted an expected round shape[44]. However, as culture progressed, the cells tended to migrate toward the surface where they would form smaller clusters if there were other cells in the surrounding. These cell clusters were more prevalent at day 14 of culture and resembled smaller versions of the 3D pellets. At this time, the cells adopted a more "spread"" morphology and, due to their lower numbers, lacked any obvious hypoxic core or cell death. These findings indicate that the cells acquired an autonomous behavior and attained a conformation that closely resembles a physiologically relevant cartilage distribution.

The final investigation included assessment of chondrogenic marker expression at both protein and mRNA transcript levels. Protein expression was assessed by immunofluorescence using SOX-9 to determine initial chondrogenesis. Positive labeling for SOX-9 was seen in both control and PeptiInk cultures on days 7 and 14. When chondrocytes are expanded in two-dimensional, it is known that they tend to lose their chondrogenic phenotype after passage 4 or 5 and behave like fibroblasts[45,46]. By assessing this early chondrogenic marker, we could assess whether the cells were retrieving their original phenotype after being placed in a 3D environment. Other studies[46] have shown that when placing previously 2D-expanded chondrocytes into a 3D environment, they started expressing SOX-9 and later chondrogenic markers. Here, we observed high intensity of intracellular nuclear SOX-9 labeling on day 7 in pellet cultures, which decreased at subsequent time points until day 14. SOX-9 labeling in PeptiInk culture was, by contrast, low on day 7 but instead increased in intensity by day 14, showing the potential induction of chondrogenic differentiation under these conditions.

Later chondrogenic markers such as collagen type II and aggrecan were also assessed. As expected, collagen type II and aggrecan were expressed in the cartilage pellet. More collagen type II appeared to be expressed at the surface of the pellet on day 7 and then increased across the matrix on day 14, which is an observation that differs from previous 3D pellet chondrocyte studies where the production of collagen type II commences at the center and spreads outward[40,41]. Aggrecan, on the other hand, seemed to be expressed all over the pellet from day 7 onward, confirming previously reported observation[43]. The hydrogel culture showed an intracellular expression of collagen type II on day 7 and a more prominent intra- and extra-cellular expression on day 14, especially in the cell cluster formations at the surface of the hydrogel. Aggrecan, on the other hand, appeared to have a lower expression on day 7 which then increased in those surface cell clusters on day 14.

These observations were further corroborated by use of qRT-PCR to assess mRNA levels of each of these three markers. Although the immunolabeling showed promising results, the nature of some of the antibodies used, such as the collagen type II polyclonal antibody, could lead to false positive results. qRT-PCR confirmed the chondrogenic behavior observed. Firstly, although not statistically significant, mRNA expression levels for all three chondrogenic markers were somewhat raised between day 7 and 14 in the 3D pellets, supporting the use of this "gold standard" system for cartilage *in vitro* chondrogenesis. Significant upregulation in levels of *COL2*, *AGC,* and *SOX9* mRNA was observed in the hydrogel culture on day 7. This supports the notion that cells respond by adopting greater chondrogenic potential in the hydrogel system during the first 7 days. The observed lack of any significant difference in mRNA levels for these chondrogenic marker transcripts in the following week (day 14) suggests that cells cultured in the hydrogel system exhibit an accelerated chondrogenic behavior.

This hydrogel system presents promising advantages such as the possibility to be used as a bioink and as a human cartilage *in vitro* model. The high expression of cartilage markers, such as collagen type II, aggrecan, and SOX-9, shows that this system also enables the chondrogenesis observed in other animal models[35]. The significant upregulation of the chosen chondrogenic mRNAs in the PeptiInk system on day 7 indicates a faster chondrogenesis when placing the human primary chondrocytes in the hydrogel system. However, the instability of the hydrogel and its fast degradation rate when mixed with cells in culture, which have already been reported[44], make it difficult to maintain the culture *in vitro* for longer than 14 days. The loss of hydrogel volume over the culture period potentially impedes the further chondrogenic development of the system into mature cartilage tissue. Further research should focus on the mechanism of degradation of these hydrogels, which has already been speculated to be cell endocytosis[44]. Additional strategies to slow down this PeptiInk degradation without disrupting the chondrogenic potential should be assessed.

Overall, our findings showed that the PeptiInk Alpha 1 culture system does promote human chondrogenesis *in vitro* and is a suitable material for 3D bioprinting. It allows for chondrocytes to survive, self-assemble and produce chondrogenic matrix proteins and markers. This animal-free alternative has great potential to bring research closer to an ethical and more sustainable platform to recreate human cartilage *in vitro*. Albeit further studies are needed to assess the feasibility of this PeptiInk to be used in long-term cultures for human cartilage *in vitro* modeling, our novel findings showed for the first time the

feasibility to use this material as a bioink and as a short-term culture platform to develop human cartilage models *in vitro.* This material, as a bioprintable material to develop human cartilage models, can be applied in personalized medicine, fundamental research, or disease modeling.

5. Conclusion

In this study, we optimized the bioprinting process of PeptiInk Alpha 1 and demonstrated its potential to manufacture human cartilage models *in vitro.* First, we assessed the printability of the material through rheological characterization and optimization of printing pressures and speeds using a 25G conical nozzle. We went on to explore the behavior that primary human chondrocytes show when encapsulated and 3D-bioprinted within Alpha 1. High cell viability, cell self-assembly, and chondrogenic protein expression at the protein and mRNA levels were observed in both the control and the PeptiInk Alpha 1 culture. This material, which can be potentially used to 3D-bioprint human cartilage tissue models *in vitro*, presents a more ethical and sustainable alternative than the current 3D-bioprinted cartilage *in vitro* models. Further work will focus on additional assessment of the chondrogenic behavior through ELISA protein quantification, improvement of the material stability for long-term cultures, and 3D bioprinting of larger constructs.

Acknowledgments

This article was written and revised only by the confirmed authors, and no other people contributed to the production of this paper.

Funding

This work was supported by the Engineering and Physical Sciences Research Council (EPSRC- EP/S021868/1) Centre for Doctoral Training.

Conflict of interest

The authors declare no conflict of interest.

Author contributions

Conceptualization: Patricia Santos-Beato, Andrew A. Pitsillides
Formal analysis: Patricia Santos-Beato
Funding acquisition: Deepak M. Kalaskar
Investigation: Patricia Santos-Beato
Supervision: Andrew A. Pitsillides, Alberto Saiani, Aline Miller, Ryo Torii, Deepak M. Kalaskar
Visualization: Patricia Santos-Beato
Writing – original draft: Patricia Santos-Beato
Writing – review & editing: Andrew A. Pitsillides, Alberto Saiani, Aline Miller, Deepak M. Kalaskar

Ethics approval and consent to participate

Not applicable.

Consent for publication

Not applicable.

Availability of data

Raw data can be accessed by contacting corresponding author

Further disclosure

Part of the entire set of findings has been presented in a conference (European Society of Biomaterials, September 2022).

References

1. Gibofsky A, 2012, Overview of epidemiology, pathophysiology, and diagnosis of rheumatoid arthritis. *Am J Manag Care*, 18(13 Suppl): S295–S302.

2. Jafarzadeh SR, Felson DT, 2018, Updated estimates suggest a much higher prevalence of arthritis in United States adults than previous ones. *Arthritis Rheumatol*, 70(2): 185–192.

   https://pubmed.ncbi.nlm.nih.gov/29178176

3. Buckwalter JA, Mow VC, Ratcliffe A, 1994, Restoration of injured or degenerated articular cartilage. *J Am Acad Orthop Surg*, 2(4): 192–201.

4. O'Hara BP, Urban JP, Maroudas A, 1990, Influence of cyclic loading on the nutrition of articular cartilage. *Ann Rheum Dis*, 49(7): 536–539.

5. Chang AA, Reuther MS, Briggs KK, *et al.*, 2012, In vivo implantation of tissue-engineered human nasal septal neocartilage constructs: A pilot study. *Otolaryngol Head Neck Surg*, 146(1): 46–52.

   https://pubmed.ncbi.nlm.nih.gov/22031592

6. Jin CZ, Cho JH, Choi BH, *et al.*, 2011, The maturity of tissue-engineered cartilage in vitro affects the repairability for osteochondral defect. *Tissue Eng Part A*, 17(23–24): 3057–3065.

   https://pubmed.ncbi.nlm.nih.gov/21736425

7. Neybecker P, Henrionnet C, Pape E, *et al.*, 2018, In vitro and in vivo potentialities for cartilage repair from human advanced knee osteoarthritis synovial fluid-derived mesenchymal stem cells. *Stem Cell Res Ther*, 9(1): 329.

   https://doi.org/10.1186/s13287-018-1071-2

8. Sanjurjo-Rodríguez C, Castro-Viñuelas R, Hermida-Gómez T, *et al.*, 2017, Human cartilage engineering in an in vitro repair model using collagen scaffolds and mesenchymal stromal cells. *Int J Med Sci*, 14(12): 1257–1262.

   https://pubmed.ncbi.nlm.nih.gov/29104482

9. Wu Y, Kennedy P, Bonazza N, *et al.*, 2021, Three-dimensional bioprinting of articular cartilage: A systematic review. *Cartilage*, 12(1): 76–92.

10. Ng WL, Chua CK, Shen YF, 2019, Print me an organ! Why we are not there yet. *Prog Polym Sci*, 97(October 1): 101145.

    https://doi.org/10.1016/j.progpolymsci.2019.101145

11. Ozbolat IT, Hospodiuk M, 2016, Current advances and future perspectives in extrusion-based bioprinting. *Biomaterials*, 76 (January 1): 321–343.

    http://dx.doi.org/10.1016/j.biomaterials.2015.10.076

12. Suntornnond R, Ng WL, Huang X, *et al.*, 2022, Improving printability of hydrogel-based bio-inks for thermal inkjet bioprinting applications via saponification and heat treatment processes. *J Mater Chem B*, 10(31): 5989–6000.

13. Ng WL, Lee JM, Zhou M, *et al.*, 2020, Vat polymerization-based bioprinting - process, materials, applications and regulatory challenges. *Biofabrication*, 12(2): 022001.

14. Sekar MP, Budharaju H, Zennifer A, *et al.,* 2021, Current standards and ethical landscape of engineered tissues-3D bioprinting perspective. *J Tissue Eng*, 12 (July 1): 20417314211027676.

15. Costantini M, Idaszek J, Szöke K, *et al.*, 2016, 3D bioprinting of BM-MSCs-loaded ECM biomimetic hydrogels for in vitro neocartilage formation. *Biofabrication*, 8(3): 035002.

    https://iopscience.iop.org/article/10.1088/1758-5090/8/3/035002

16. Daly AC, Critchley SE, Rencsok EM, *et al.*, 2016, A comparison of different bioinks for 3D bioprinting of fibrocartilage and hyaline cartilage. *Biofabrication*, 8(4): 045002.

    https://iopscience.iop.org/article/10.1088/1758-5090/8/4/045002

17. Duchi S, Onofrillo C, O'Connell CD, *et al.*, 2017, Handheld co-axial bioprinting: Application to in situ surgical cartilage repair. *Sci Rep*, 7(1): 5837.

18. Gao G, Schilling AF, Hubbell K, *et al.*, 2015, Improved properties of bone and cartilage tissue from 3D inkjet-bioprinted human mesenchymal stem cells by simultaneous deposition and photocrosslinking in PEG-GelMA. *Biotechnol Lett*, 37(11): 2349–2355.

19. Levato R, Visser J, Planell JA, *et al.*, 2014, Biofabrication of tissue constructs by 3D bioprinting of cell-laden microcarriers. *Biofabrication*, 6(3): 035020.

    https://iopscience.iop.org/article/10.1088/1758-5082/6/3/035020

20. Levato R, Webb WR, Otto IA, *et al.*, 2017, The bio in the ink: Cartilage regeneration with bioprintable hydrogels and articular cartilage-derived progenitor cells. *Acta Biomater*, 61 (October 1): 41–53.

21. Mouser VHM, Melchels FPW, Visser J, *et al.*, 2016, Yield stress determines bioprintability of hydrogels based on gelatin-methacryloyl and gellan gum for cartilage bioprinting. *Biofabrication*, 8(3): 35003.

22. O'Connell CD, Di Bella C, Thompson F, *et al.*, 2016, Development of the Biopen: A handheld device for surgical printing of adipose stem cells at a chondral wound site. *Biofabrication*, 8(1): 15019.

23. Zhu W, Cui H, Boualam B, *et al.*, 2018, 3D bioprinting mesenchymal stem cell-laden construct with core-shell nanospheres for cartilage tissue engineering. *Nanotechnology*, 29(18): 185101.

24. Abbadessa A, Mouser VHM, Blokzijl MM, *et al.*, 2016, A synthetic thermosensitive hydrogel for cartilage bioprinting and its biofunctionalization with polysaccharides. *Biomacromolecules,* 17(6): 2137–2147.

    https://pubs.acs.org/doi/10.1021/acs.biomac.6b00366

25. Wasyłeczko M, Sikorska W, Chwojnowski A, 2020, Review of synthetic and hybrid scaffolds in cartilage tissue engineering. *Membranes,* 10(11): 348.

    https://pubmed.ncbi.nlm.nih.gov/33212901

26. Popov A, Malferrari S, Kalaskar DM, 2017, 3D bioprinting for musculoskeletal applications. *J 3D Print Med*, 1(3): 191–211.

    https://www.futuremedicine.com/doi/10.2217/3dp-2017-0004

27. OECD, 2018, *Guidance Document on Good In Vitro Method Practices (GIVIMP)*, Vol. 1, OECD Publishing, Paris, 1–264.

    https://www.oecd-ilibrary.org/docserver/9789264304796-en.pdf?expires=1621462493&id=id&accname=guest&checksum=4EA871101E844045CE8D833D9DFADC25%0A

    https://www.oecd-ilibrary.org/environment/guidance-document-on-good-in-vitro-method-practices-givimp_9789264304

28. Ligorio C, Hoyland JA, Saiani A, 2022, Self-assembling peptide hydrogels as functional tools to tackle intervertebral disc degeneration. *Gels*, 8(4).

    https://www.mdpi.com/2310-2861/8/4/211

29. Mujeeb A, Miller AF, Saiani A, Gough JE. 2013; Self-assembled octapeptide scaffolds for in vitro chondrocyte culture. 9(1):4609–17. 2013. Acta Biomater [Internet]. Available from:

    http://dx.doi.org/10.1016/j.actbio.2012.08.044

30. Wan S, Borland S, Richardson SM, *et al.*, 2016, Self-assembling peptide hydrogel for intervertebral disc tissue engineering. *Acta Biomater*, 46(December 1): 29–40.

    https://www.sciencedirect.com/science/article/pii/S1742706116305062

31. Raphael B, Khalil T, Workman VL, *et al.*, 2017, 3D cell bioprinting of self-assembling peptide-based hydrogels. *Mater Lett,* 190: 103–6.

32. Gatenholm B, Lindahl C, Brittberg M, *et al.*, 2020, Collagen 2A type B induction after 3D bioprinting chondrocytes in situ into osteoarthritic chondral tibial lesion. *Cartilage*, 13(December 1): 1–15.

http://journals.sagepub.com/doi/10.1177/1947603520903788

33. Yang IH, Kim SH, Kim YH, *et al.*, 2004, Comparison of phenotypic characterization between "alginate bead" and "pellet" culture systems as chondrogenic differentiation models for human mesenchymal stem cells. *Yonsei Med J,* 45: 891–900.

http://www.ncbi.nlm.nih.gov/pubmed/15515201

34. Yeung P, Cheng KH, Yan CH, *et al.*, 2019, Collagen microsphere based 3D culture system for human osteoarthritis chondrocytes (hOACs). *Sci Rep*, 9(1): 1–14.

http://dx.doi.org/10.1038/s41598-019-47946-3

35. Ligorio C, Zhou M, Wychowaniec JK, *et al.*, 2019, Graphene oxide containing self-assembling peptide hybrid hydrogels as a potential 3D injectable cell delivery platform for intervertebral disc repair applications. *Acta Biomater*, 92: 92–103.

https://doi.org/10.1016/j.actbio.2019.05.004

36. Lemarié L, Anandan A, Petiot E, *et al.*, 2021, Rheology, simulation and data analysis toward bioprinting cell viability awareness. *Bioprinting*, 21(December 2020): e00119.

https://linkinghub.elsevier.com/retrieve/pii/S2405886620300464

37. Schmitz C, Potekhina E, Belousov VV, *et al.,* 2021, Hypoxia onset in mesenchymal stem cell spheroids: monitoring with hypoxia reporter cells. *Front Bioeng Biotechnol*, 9(February).

38. Caron MMJ, Emans PJ, Coolsen MME, *et al.*, 2012, Redifferentiation of dedifferentiated human articular chondrocytes: Comparison of 2D and 3D cultures. *Osteoarthr Cartil*, 20(10): 1170–1178.

http://dx.doi.org/10.1016/j.joca.2012.06.016

39. Haseeb A, Kc R, Angelozzi M, *et al.*, 2021, SOX9 keeps growth plates and articular cartilage healthy by inhibiting chondrocyte dedifferentiation/osteoblastic redifferentiation. *Proc Natl Acad Sci*, 118(8): e2019152118.

https://www.pnas.org/doi/abs/10.1073/pnas.2019152118

40. Schon BS, Schrobback K, Van Der Ven M, *et al.*, 2012, Validation of a high-throughput microtissue fabrication process for 3D assembly of tissue engineered cartilage constructs. *Cell Tissue Res*, 347(3): 629–642.

41. Bosnakovski D, Mizuno M, Kim G, *et al.*, 2004, Chondrogenic differentiation of bovine bone marrow mesenchymal stem cells in pellet cultural system. *Exp Hematol*, 32(5): 502–509.

42. Griffin MF, Ibrahim A, Seifalian AM, *et al.*, 2017, Chemical group-dependent plasma polymerisation preferentially directs adipose stem cell differentiation towards osteogenic or chondrogenic lineages. *Acta Biomater*, 50: 450–61.

http://dx.doi.org/10.1016/j.actbio.2016.12.016

43. Zhang Z, McCaffery JM, Spencer RGS, *et al.*, 2004, Hyaline cartilage engineered by chondrocytes in pellet culture: Histological, immunohistochemical and ultrastructural analysis in comparison with cartilage explants. *J Anat*, 205(3): 229–237.

44. Faroni A, Workman VL, Saiani A, *et al.*, 2019, Self-assembling peptide hydrogel matrices improve the neurotrophic potential of human adipose-derived stem cells. *Adv Healthc Mater*, 8(17).

45. Benya P, 1982, Dedifferentiated chondrocytes reexpress the differentiated collagen phenotype when cultured in agarose gels. *Cell,* 30(1): 215–224.

https://doi.org/10.1016%2F0092-8674%2882%2990027-7

46. Lemare F, Steimberg N, Le Griel C, *et al.*, 1998, Dedifferentiated chondrocytes cultured in alginate beads: Restoration of the differentiated phenotype and of the metabolic responses to interleukin- 1β. *J Cell Physiol*, 176(2): 303–313.